Eur. Radiol. (2001) 11: 2319–2331
DOI 10.1007/s003300100908

CONTRAST MEDIA

Yi-Xiang J. Wang
Shahid M. Hussain
Gabriel P. Krestin

Superparamagnetic iron oxide contrast agents: physicochemical characteristics and applications in MR imaging

Received: 27 November 2000
Revised: 7 March 2001
Accepted: 12 March 2001
Published online: 3 May 2001

Y.-X. J. Wang · S. M. Hussain · G. P. Krestin (✉)
Department of Radiology, Erasmus University Medical Center–Dijkzigt, Dr. Molewaterplein 40, 3015 GD Rotterdam, The Netherlands
E-mail: Krestin@rond.azr.nl
Phone: +31-10-4634044
Fax: +31-10-4634033

Abstract Superparamagnetic iron oxide MR imaging contrast agents have been the subjects of extensive research over the past decade. The iron oxide particle size of these contrast agents varies widely, and influences their physicochemical and pharmacokinetic properties, and thus clinical application. Superparamagnetic agents enhance both T1 and T2/T2* relaxation. In most situations it is their significant capacity to reduce the T2/T2* relaxation time to be utilized. The T1 relaxivity can be improved (and the T2/T2* effect can be reduced) using small particles and T1-weighted imaging sequences. Large iron oxide particles are used for bowel contrast [AMI-121 (i.e. Lumirem and Gastromark) and OMP (i.e. Abdoscan), mean diameter no less than 300 nm] and liver/spleen imaging [AMI-25 (i.e. Endorem and Feridex IV, diameter 80–150 nm); SHU 555A (i.e. Resovist, mean diameter 60 nm)]. Smaller iron oxide particles are selected for lymph node imaging [AMI-227 (i.e. Sinerem and Combidex, diameter 20–40 nm)], bone marrow imaging (AMI-227), perfusion imaging [NC100150 (i.e. Clariscan, mean diameter 20 nm)] and MR angiography (NC100150). Even smaller monocrystalline iron oxide nanoparticles are under research for receptor-directed MR imaging and magnetically labeled cell probe MR imaging. Iron oxide particles for bowel contrast are coated with insoluble material, and all iron oxide particles for intravenous injection are biodegradable. Superparamagnetic agents open up an important field for research in MR imaging.

Keywords Contrast agent · Iron oxide · MR imaging · Superparamagnetism

Introduction

Superparamagnetic iron oxide (SPIO) MR imaging contrast agents are extremely strong enhancers of proton relaxation. These superparamagnetic agents have been the subject of extensive research over the past decade. While many of them are still in clinical trial or experimental study stages, a few products have been marketed [1, 2, 3]. SPIO agents include a wide range of preparations whose physico-chemical properties differ greatly. This article reviews these agents' physicochemical properties, bio-distribution and clinical applications, which include bowel contrast, liver and spleen imaging, lymph node imaging, bone marrow imaging, perfusion imaging and MR angiography. Receptor-directed imaging and magnetically labeled cell probe MR imaging are also under experimental study [4, 5, 6]. The clinical applications of various specific SPIO agents indicated in this review are based on the most recent literature, however their applications will be extended upon further research. The agents exploiting the paramagnetic property of the soluble iron ion for contrast are not reviewed in this article.

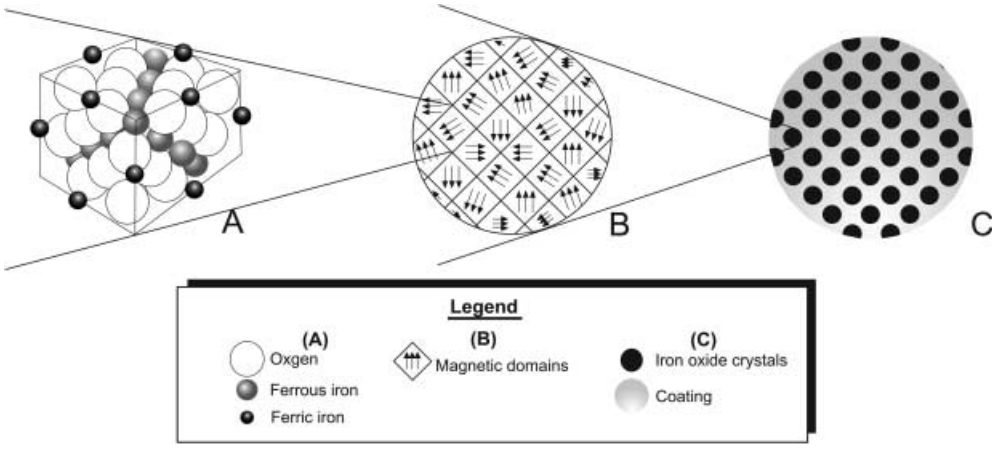

Fig. 1 Schematic representation of **A** spinal crystal structure for superparamagnetic iron oxide *(SPIO)* domain; **B** SPIO crystal with multiple magnetic domains of random orientation and **C** complete SPIO contrast agent particle, with multiple SPIO crystals and coating materials

Physicochemical characteristics of superparamagnetic iron oxide agents

Superparamagnetic iron oxide crystalline structures have the general formula $Fe_2^{3+}O_3M^{2+}O$, where M^{2+} is a divalent metal ion such as iron, manganese, nickel, cobalt, or magnesium. SPIO is magnetite when the metal ion (M^{2+}) is ferrous iron (Fe^{2+}) (Fig. 1A). Superparamagnetism occurs when crystal-containing regions of unpaired spins are sufficiently large that they can be regarded as thermodynamically independent, single-domain particles. These single-domain particles are named magnetic domains (Fig. 1B). Such a magnetic domain has a net magnetic dipole that is larger than the sum of its individual unpaired electrons [7, 8]. In the absence of an applied magnetic field, such magnetic domains are free to rotate from thermal motion, and are randomly oriented with no net magnetic field (Fig. 2A). An external magnetic field can cause the magnetic dipoles of the magnetic domains to reorient, analogous to paramagnetic materials (Fig. 2B). The *magnetic moments*[1] of such magnetic domains reflect interacting unpaired electrons; the resultant magnetic moment is much greater than that of a paramagnetic substance, and the specific *magnetic susceptibilities*[2] of these particulates can significantly exceed those of corresponding soluble paramagnetic species because of this magnetic ordering [7, 8]. Superparamagnetic substances lack remnant magnetization when the external magnetic field is terminated, as the magnetic moment of the individual magnetic domains loose their collective orientation and the net magnetic moment becomes zero. That means SPIO agents will not self-aggregate due to magnetic attraction. Superparamagnetism has an obligatory crystalline nature; superparamagnetic agents will therefore necessarily be particulate [1].

Both T1 and T2/T2* relaxation processes are shortened by SPIO. MR contrast agents' *relaxivity*[3] is typically measured at 37 °C and 0.47 T. The T2 relaxivity of 100 $mmol^{-1}\,l\,s^{-1}$ and T1 relaxivity of 30 $mmol^{-1}\,l\,s^{-1}$ of typical SPIO agent are substantially larger than the relaxivity of paramagnetic molecules such as Gd-DTPA (T2 relaxivity of 6 $mmol^{-1}\,l\,s^{-1}$ and T1 relaxivity of 4 $mmol^{-1}\,l\,s^{-1}$) [9]. The observed effects on signal intensity depend on various factors, including particle composition, particle size, concentration of particles within a given imaging voxel, and data acquisition parameters. Accordingly the clinical doses of SPIO agents may vary with imaging sequences. The magnetic field applied has also a non-linear influence on the signal, however this property is not so important in clinical practice [1]. In most situations, it is SPIO agents' significant capacity to reduce the MRI signal to be utilized, which can be emphasized by using spin echo sequences with a longer echo time (TE) and by using gradient-echo sequences. However, when particulates of smaller sizes are used and T1W sequences are chosen, their T1 relaxation shortening property is emphasized [10, 11]. Sometimes the decrease in signal intensity caused by SPIO agents can be so pronounced that it can cause distortion or obliteration of organ boundaries. This effect of magnetic susceptibility, also called "blooming", can be mitigated by specifying data acquisition parameters that have less T2 or T2* dependence.

The typical synthesis of SPIO agents involves controlled precipitation of iron oxide in an aqueous solution of ferrous salt, ferric salt and coating material

[1] Magnetic moment is a measurement of the magnetic properties of a dipole, which interacts with an applied magnetic field such as a bar magnet. Magnetic moment is one factor that determines the efficiency of proton relaxation enhancement of an agent.

[2] Magnetic susceptibility is the tendency of a substance to become magnetized or to distort an applied magnetic field. Magnetic susceptibility causes signal loss and, when severe, causes geometric distortion on MR images.

[3] Relaxivity is the measurement of the efficiency by which the MR contrast agents enhance the proton relaxation rates.

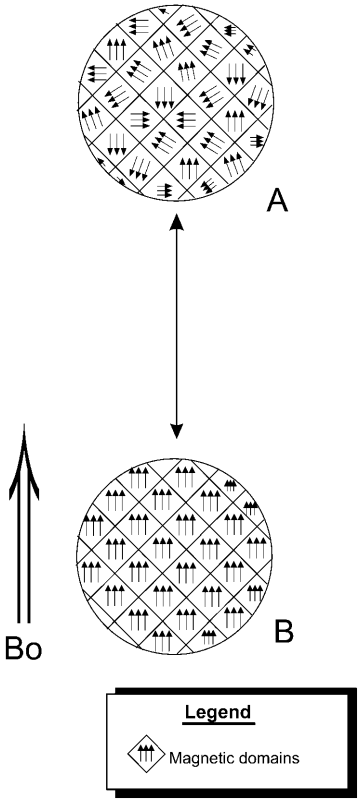

Fig. 2 **A** Superparamagnetic iron oxide *(SPIO)* crystal in the absence of an external magnetic field; the orientation of the magnetic domains is random. **B** An external magnetic field (B_0) causes the magnetic domains of the SPIO crystal to reorient according to the B_0

(dextran or others) by addition in drops of an alkaline solution while active stirring or sonication is applied. The SPIO agents are then isolated by differential centrifugation and dialyzing [1, 10, 12, 13]. SPIO agents are thus often composed of both an active SPIO component (iron oxide crystals, which vary in size from agent to agent and also depend on the measurement technique; their sizes are generally between 4 and 10 nm), and a coating material (Fig. 1C). The total particle size (including the iron oxide crystals and the coating material) in solution can be larger than the dry size, due to the absorbed, hydrated coating dextran layer. To describe the particle size, usually *hydrodynamic diameter* is used. Hydrodynamic diameter is derived from dynamic light scattering techniques which calculate average solution particle sizes by monitoring the diffusion characteristics of the particles in solution. The resulting solution particle sizes are the diameters of hypothetical spheres with the same diffusion coefficients as the SPIO aggregates with their adsorbed, solvated coating materials. The mean diameters of injectable particles vary from 1 μm to less than 10 nm [1, 5, 14, 15]. Since the injected particles are much smaller than erythrocytes (approximately 7 μm in diameter), they easily traverse capillary beds.

The size of the particle, the charge and the nature of the coating determine the stability, bio-distribution and metabolism of SPIO agents [16]. Although most superparamagnetic particles are coated with dextran or dextran derivatives, they can also be coated by other composites, such as starch, albumin, and arabinogalactose. These composites are bio-compatible, thus permitting safe intravenous administration and ready biodegradability. Since SPIO particle uptake into the reticuloendothelial system (RES) is related to protein absorption on the particle surface and subsequent opsonization, minimizing the particle surface will result in a decreased protein absorption, which reduces particle phagocytosis, finally resulting in a significant increase in plasma half-life and wider bio-distribution [17].

As SPIO agents degrade, the iron enters the plasma iron pool and is subsequently incorporated into red cell production and other natural uses of iron. Eventually it is secreted from the body as the body iron stores turn over. The smaller size of particles accelerates degradation of SPIO into paramagnetic forms of iron. The amount of iron oxide that would be required for clinical MR imaging is small compared with the physiological iron stores [1, 18]. Compared with other MR agents, SPIO agents' toxicity is low. Extensive toxicity studies in animals have disclosed no acute toxicity or chronic injury at doses greater than 100 times the clinical effective dose [19].

Classification of superparamagnetic iron oxide agents

Superparamagnetic iron oxide contrast agents include oral (large) SPIO agents, standard SPIO (SSPIO) agents, ultrasmall SPIO (USPIO) agents and monocrystalline iron oxide nanoparticle (MION) agents. The former three kind of agents have been approved for clinical application or are being clinically tested, under various generic names and trade names (Tables 1 and 2). MION agents are still at the experimental study stage. Injectable SPIO agents are colloidal suspensions containing invisible particles. These particles will remain in suspension and do not settle out from the solution because the energy of Brownian motion largely surpasses the strength of gravity, and, in an external magnetic field, also that of magnetic attraction. To ensure no aggregated particles will be injected, some SPIO agents are introduced via a 5 μm filter. Larger particles in temporary dispersion, such as some agents for bowel contrast, may settle spontaneously upon storage [1].

Table 1 The generic and trade names of superparamagnetic iron oxide *(SPIO)* agents

Agent	Classification	Generic name	Trade name	Developing company	Status
AMI-121	Oral SPIO	Ferumoxsil	Lumirem Gastromark	Guerbet Advanced Magnetics	Approved Approved
OMP	Oral SPIO		Abdoscan	Nycomed	Approved
AMI-25	SSPIO	Ferumoxide	Endorem Feridex IV	Guerbet Berlex Laboratories	Approved Approved
SHU 555A	SSPIO		Resovist	Schering	Phase 3 completed
AMI-277	USPIO	Ferumoxtran	Sinerem Combidex[a]	Guerbet Advanced Magnetics	Phase 3 Phase 3
NC100150	USPIO		Clariscan	Nycomed	Phase 3

[a]Also tested as BMS 180549 and Code 7227

Table 2 Properties and applications of some superparamagnetic iron oxide *(SPIO)* agents. The main references for this table are: for AMI-121 [20]; for OMP [1]; for AMI-25 [2, 22]; for SHU 555A [2, 18, 78]; for AMI-227 [25, 26, 27, 29]; for NC100150 [19, 24]

Agent	Particle size	Target organs	Dose[a]	Mode of administration
AMI-121	300 nm	GI lumen	1.5–3.9 $mmol^{-1}$ l Fe 400–600 ml	p.o.
OMP	3.5 μm	GI lumen	0.5 g/l 400–600 ml	p.o.
AMI-25	80–150 nm	Liver/spleen	15 μmol Fe/kg	Slow infusion
SHU 555A	62 nm	Liver/spleen Perfusion[b] MRA[b]	8 μmol Fe/kg 4–16 μmol Fe/kg 10 μmol Fe/kg	Bolus injection Bolus injection Bolus injection
AMI-277	20–40 nm	Lymph nodes MRA[c]	30–45 μmol Fe/kg 14–30 μmol Fe/kg	Slow infusion Slow infusion
NC100150	20 nm	Perfusion MRA	7 μmol Fe/kg 50–100 μmol Fe/kg	Bolus injection Bolus injection

[a]The doses of SPIO agents may vary with imaging sequences and target organs: highly T2/T2*-weighted sequences require a smaller dose, T2* gradient echo sequences require a smaller dose than T2W SE sequences. Please refer to the information provided by the vendors and up-dated references for exact dosing

[b]Perfusion imaging and MR angiography are not the primary goals of SHU 555A. However, when properly administered and imaged, perfusion images and MR angiographic images can be obtained with SHU 555A

[c]MR angiography is not the primary goal of AMI-277. However, when properly administered and imaged, MR angiographic images can be obtained with AMI-277

Oral superparamagnetic iron oxide agents

Oral SPIO preparations usually contain larger particles than do injectable agents. They are coated with a non-biodegradable and insoluble matrix (siloxane for AMI-121 and polystyrene for OMP), and suspended in viscosity-increasing agents (usually based on ordinary food additives, such as starch and cellulose) [1, 20]. These preparations can prevent the ingested iron from being absorbed, and particles from aggregating, and improve homogeneous contrast distribution throughout the bowel. If SPIO particle aggregating occurs, magnetic susceptibility artifact may result, especially when high field strength and gradient echo pulse sequences are used. Two oral SPIO agents (AMI-121 and OMP) have been tested in clinical trials. Oral SPIO agents are used as negative contrast agents, i.e. they decrease signal on T2W images.

AMI-121 (Lumirem by Guerbet and Gastromark by Advanced Magnetics) is composed of crystal of approximately 10 nm; the hydrodynamic diameter is approximately 300 nm. The relaxivities are 72 and 3.2 $mmol^{-1}$ l s^{-1} respectively, for T2 and T1 relaxivity. The recommended concentration is 1.5–3.9 $mmol^{-1}$ l Fe [20].

OMP (Abdoscan, Nycomed) is composed of crystal of below 50 nm. The total particle size is 3.5 μm. The particles contain 25 % iron oxide w/w, the concentration of OMP is 0.5 g/l [1].

Oral SPIO is normally administered over 30–60 min, with a volume of 900 ml for contrast enhancement of the whole abdomen, and 400 ml for imaging of the upper abdomen. Oral SPIO suspensions are well-tolerated by the patients: the iron is not absorbed and the intestinal mucosal membrane is not irritated [1, 20].

Standard superparamagnetic iron oxide agents

Standard superparamagnetic iron oxide agents are easily sequestered by the RES cells in the liver and spleen upon intravenous administration. Intravenous administration of SPIO failed to localize within lymph nodes in sufficient amounts to be imaged, though interstitial administration of SSPIO can lead to lymph node enhancement on T2/T2*W imaging [21]. SSPIO agents have a high *T2 relaxivity/T1 relaxivity ratio*, i.e. have a marked T2 relaxation effect [9]. Many SSPIO preparations have been developed. Currently AMI-25 is approved for clinical use, SHU 555A completed phase 3 trials and clinical approval is expected very soon.

AMI-25 (Endorem by Guerbet and Feridex by Berlex Laboratories) is coated with dextran, the iron oxide crystal is 4.8–5.6 nm, and the hydrodynamic diameter is 80–150 nm. The T2 and T1 relaxivities are 98.3 and 23.9 $mmol^{-1}\,l\,s^{-1}$ respectively [22]. AMI-25 efficiently accumulates in the liver (approximately 80 % of the injected dose) and spleen (5–10 % of the injected dose) within minutes of administration; the blood half-life is 6 min [22]. Peak concentrations of iron were found in liver after 2 h and in the spleen after 4 h. Iron is slowly cleared from liver (half-life, 3 days) and spleen (half-life, 4 days) [22]. AMI-25 preparation is usually not bolus-injected because of cardiovascular side effects and lumbar pain. The recommended mode of administration is a dose of 15 μmol Fe/kg in 100 ml of glucose 5 % and a biphasic infusion (2 ml/min over 10 min and 4 ml/min over 20 min). AMI-25 allows a wide scan window for T2/T2*W imaging (0.5~6 h after administration) [2].

SHU 555A (Resovist, Schering AG) is a SSPIO characterized by a carbodextran rather than dextran coating. The crystal of SHU 555A is 4.2 nm and the hydrodynamic diameter is 62 nm. The T2 and T1 relaxivities are 151.0 and 25.4 $mmol^{-1}\,l\,s^{-1}$ respectively. Unlike AMI-25, Resovist does not show side effects after rapid intravenous injection (performed by preloading SHU 555A into a connecting intravenous line and flushing the line with 10 ml saline for 3 s). A dose of 8 μmol Fe/kg is the recommended quantity for liver T2W imaging at retention phase (after the SPIO particles have been trapped by the phagocytes), which can be scanned 30 min after administration [18]. Due to its smaller size and thus stronger T1 relaxation property, SHU 555A has also been used for T1W imaging and MR angiography. Dynamic T1W MR imaging following bolus infusion of SHU 555A mimics signal changes caused by gadolinium chelates [2]. Significant vessel T1 relaxation enhancement can be achieved at a dose of 10 μmol Fe/kg [2].

Ultrasmall superparamagnetic iron oxide agents

The prototype of USPIO was developed by Weissleder et al. [10]. The hydrodynamic diameter is 11.4 ± 6.3 nm. The T2 and T1 relaxivities are 44.1 and 21.6 $mmol^{-1}\,l\,s^{-1}$ respectively. The *T2 relaxivity/T1 relaxivity Ratio* was approximately 2, lower than that of SSPIO particles. The blood half-life of the T1 effects is 80 min [10]. The small size and prolongation of the blood half-life enable this agent to cross the capillary wall and have more widespread tissue distribution, leading to extensive uptake by the RES of lymph nodes and bone marrow. USPIO can be delivered to the interstitium by non-specific vesicular transport and through transendothelial channels. Once in the interstitium, USPIO particles are cleared by draining lymphatic vessels and transported to lymph nodes, thus making them suitable for T2/T2*W MR lymphography. Due to their long blood half-life, low concentration of USPIO agents can be used for T1W MR angiography (high concentrations may leads to signal loss due to their T2-shortening effects). Two USPIO agents, AMI-227 and NC100150, are currently under clinical phase 3 trials [23, 24].

AMI-227 (Sinerem by Guerbet and Combidex by Advanced Magnetics) is composed of a crystalline core of 4–6 nm surrounded by dextran coating. The hydrodynamic diameter is 20–40 nm. Their relaxivity is similar to the prototype of USPIO [9, 23]. Despite the slightly larger size of AMI-277 compared with the prototype USPIO, AMI-277 has a much longer plasma half-life due to improved coating. In humans, the blood pool half-life of plasma relaxation times is calculated to be more than 24 h [23]. Because of its long blood half-life and significant T1 relaxation effects, AMI-277 can be used as blood pool agent during the early phase of intravenous administration [25, 26, 27]. In the late phase, AMI-277 is suitable for the evaluation of RES in the body, particularly in lymph nodes [28, 29]. A dose of 13.8–29.2 μmol Fe/kg is used for MR angiography. The clinical dose of AMI-277 for MR lymphography can range from 29.2 to 44.7 μmol Fe/kg; usually with fast spin echo (SE) sequences a high dose is used and with gradient echo sequences a low dose is used [30]. AMI-277 is not bolus-injected, rather, it should be infused slowly over a period of 30 min to avoid hypotensive reactions or acute lumbar pain.

NC100150 (Clariscan, Nycomed) is a type of USPIO developed for MR angiography and perfusion study [31]. It has an iron oxide core of 5–7 nm diameter, and a carbohydrate-polyethylene glycol coating. The total particle is 20 nm. The T2 and T1 relaxivities are 35 and 20 $mmol^{-1}\,l\,s^{-1}$ respectively. The vascular half-life is dose-dependent and ranges from 3 to 4 h [24, 31]. The low value of *T2 relaxivity/T1 relaxivity Ratio* (1.8) of this formulation is favorable for T1 relaxation enhancement. The agent has been shown to be safe in humans when

administered intravenously as a bolus in doses up to 172 μmol Fe/kg. The optimal dose for MR angiography is 50–100 μmol Fe/kg; it allows prolonged delineation (> 45 min) of vasculatures as observed by MR angiography [31]. Brain T2*W perfusion study has been tested at a dose of 7 μmol Fe/kg [19].

Currently, Schering AG is also developing a USPIO, SHU 555C, with a mean diameter of ≤20 nm. SHU 555C is bolus-injectable and can be used for MR angiography and perfusion imaging. [32, 33]

Monocrystalline iron oxide nanoparticles

Monocrystalline iron oxide nanoparticles differ from other iron oxide preparations in their monocrystallinity, which fulfills the criteria for receptor-directed MR imaging and magnetically labeled cell probe MR imaging agent due to its very small size (2.8 ± 9 nm). MIONs can easily pass through capillary endothelium while retaining superparamagnetism [14, 15]. Initial studies used gadolinium chelates as receptor-directed agent but very high levels of this contrast agent were needed to significantly reduce proton relaxation times, which make gadolinium chelates less practicable. MIONs provide higher magnetic susceptibility (two to three orders of magnitude) than gadolinium. It has been stated that in vivo detection with MR imaging is possible at concentration as low as 1 μg Fe/g tissue [14, 15]. Targeted MR imaging with MION is still in the experimental stage, but may prove to be a powerful tool for cellular and molecular MR imaging in the future.

Application of superparamagnetic iron oxide agents for bowel contrast

MR bowel contrast is better done with negative agents rather than positive agents [3]. Negative bowel agents decrease the extent of noises and motion artifacts related to bowel peristalsis, but on the other hand, positive agents increase these noises and artifacts, especially with slower scanners [1]. The use of negative oral SPIO agents giving rise to a signal void from the intestinal loops may reinforce the visualization of intra-abdominal lesions, both on T2W images, where the lesions often appear hyperdense, and in T1W images in association with injection of a gadolinium chelate.

Bowel opacification may be helpful in certain specific circumstances, such as in the evaluation of pancreatic diseases and in the delineation of bowel pelvic abnormalities. Negative oral SPIO agents can also improve the quality of images obtained with MR urography and MR cholangiopancreatography, by eliminating unwanted signals from fluid contained in adjacent bowel loops [34].

Application of superparamagnetic iron oxide agents in reticuloendothelial system imaging

After intravenous administration, SSPIO and USPIO particles are taken up by RES cells; their value in liver and lymph node MR imaging has been well-established. Due to their prominent RES cell phagocytosis and T2 relaxivity, SSPIO agents show a stronger signal loss in the liver and spleen than do USPIOs. However, high doses of smaller SPIOs can still achieve a comparable enhancement for liver and spleen imaging as obtained by SSPIOs [35]. The diagnostic utilities of SPIO-enhanced MR imaging for other normal tissues and lesions with phagocyte involvement are also under investigation.

Liver and spleen imaging

After intravenous administration, SSPIOs are cleared from the blood within minutes, rapidly accumulating in the RES cells of liver and spleen. With T2W sequences the presence of SPIO particles decreases signal intensity of normal parenchyma of liver and spleen. Focal lesions without RES cells usually maintain nearly the same signal intensity before and after the administration of the SSPIO. There is consensus now that SSPIO-enhanced MR imaging significantly increases tumor-to-liver contrast, and improves lesion conspicuity and detectability on T2W images [36]. It has been reported that ferumoxide-enhanced MR imaging has a sensitivity for metastatic lesion detection of 95 % [37]. In a large multicenter trial, additional liver lesions were identified on 27 % of ferumoxide-enhanced images compared with unenhanced scans [38]. However, it should be noted that the presence of phagocytic cells within early stages of hepatocellular carcinoma might cause enhancement comparable with adenomatous hyperplasia.

Efforts exploiting smaller SPIOs' T1 effects during liver MR imaging have also been reported. Dynamic T1W perfusion imaging of SHU 555A and AMI-277 provides information of the vascularity of liver solid lesions similar to that by Gd chelates, e.g. hypervascular hepatocellular lesions may demonstrate an initial signal increase [2, 39]. MR angiography of the liver artery and portal venous system can be performed with these agents during the accumulation phase (when SPIO particles are being trapped by phagocytes in the organs), showing increased vascular signal by a suppression of background liver signal [40].

Though hemangiomas do not contain Kupffer cells, with both distribution phase images (while contrast agents remain in circulation) and retention phase images, hemangiomas demonstrated greater SPIO uptake than malignant neoplasms. Due to the SPIO's T1 relaxivity, on distribution phase T1W SE images hemangiomas may show signal enhancement and become bright

[41]. The degree of enhancement on T1W images and drop in signal intensity on T2W images were significantly higher in hemangiomas than in malignant liver masses [42, 43].

Experimental studies showed SPIO-enhanced MR imaging might be valuable in assessing hepatic function via observation of phagocytotic activity. SPIO-enhanced MR imaging was compared with rat models of allogeneic and syngeneic liver transplantation. Uptake of SPIO was decreased in the acutely rejecting livers but was normal in the syngeneic transplantation model [44]. SPIO-enhanced MR imaging can detect the range and extent of liver injury a few days after irradiation [45]. However, it was also reported that the dose-dependency and rate of decay of efficacy of SPIO in cirrhosis were similar to those in normal liver [46, 47]. Further studies are warranted to establish finally the role of SPIO-enhancement in assessing liver function.

SPIO-enhanced MR imaging is also able to improve the detection of diffuse and focal splenic disease [48].

Lymph node imaging

The diagnosis of lymph node metastases is difficult without proper contrast agents. Metastatic nodes vary in diameter, and signal intensities of metastatic nodes do not differ from those of normal nodes. Normal-sized metastatic nodes cannot be differentiated from large reactive nodes. With SPIO-enhanced MR imaging, metastatic nodes can be differentiated from normal nodes based on the absence of signal intensity change between pre- and post-contrast scans [29].

After intravenous administration, USPIO is taken up by macrophages within lymph nodes and therefore reduces the signal of normal functioning nodes on T2/T2*W images. Metastatic nodes that are partially or completely replaced by tumor cells do not possess the same levels of phagocytotic activity as normal nodes, and maintain the same signal intensity on post-contrast MR images. With SPIO-enhanced MR imaging, a sensitivity of 95 % and specificity of 84 % have been reported for diagnosing tumor-bearing lymph nodes [28]. Normal-sized metastatic nodes, which would have been missed if size criteria alone had been used, can be detected [49]. The rare false-positive results had been reported to be related to well-encapsulated necrotic nodes, reactive follicular hyperplasia of lymph node with scarce macrophages, and heterogeneous microstructural distribution of iron oxide particles within the lymph node [29]. Differentiation between reactive and tumor-bearing lymph nodes is also possible: reactive lymph nodes contain functional macrophages and can be enhanced [50].

The optimal time for post-contrast imaging is 24 h after SPIO administration [30]. Because the USPIO is administered intravenously, lymph nodes through the entire body can be imaged with a single injection.

To administer these agents by subcutaneous or intramuscular injection is also feasible. Under these conditions lymphatic drainage transports the contrast agent to the lymph nodes close to the injection site.

Bone marrow imaging

Bone marrow MR imaging has a high sensitivity for detection of marrow lesions. However focal lesion detection can be difficult in situations in which the uninvolved marrow is richly cellular, such as in infants and children, and in adults with red marrow hyperplasia. Marrow areas representing islands of regenerating red marrow may mimic focal marrow lesions. The administration of USPIO that could assess bone marrow phagocytic activity is useful in differentiating phagocytic normal marrow from abnormal marrow, where phagocytic function is altered.

Experimental studies have shown that bone marrow RES uptake of the intravenously injected USPIO is sufficient to reduce the signal of bone marrow MR imaging. Maximum decrease in relaxation times of marrow occurred within 1–24 h after intravenous administration. USPIO-enhanced MR imaging improves detection of smaller tumors and allows differentiation of tumor deposits from islands of hyperplastic or normal red marrow [51]. USPIO may accumulate in a zone of inflammation outside the tumor margin. A hypointense zone outlined the tumor margins on post-contrast T2W imaging improved visualization of the soft tissue component of the larger lesions [52, 53].

Radiation-induced alterations of the blood-bone marrow barrier and the RES activity can also be studied with USPIO-enhanced MR imaging. The bone marrow enhancement increases significantly following irradiation, corresponding to alterations of the endothelial lining of the bone marrow sinusoids and increased RES activity [54].

It had been reported that AMI-25, a type of SSPIO, could also decrease the relaxation times of human normal vertebral marrow. It was suggested that the amount of small particles contained in AMI-25 are phagocytosed by the marrow RES [55].

Macrophage activity in neoplasms of the hematopoietic system can persist despite marrow infiltration, and the enhanced pattern of these lesions may be the same as normal marrow.

Reticuloendothelial system imaging at other sites

Experimental studies showed SPIO-enhanced MR imaging might increase the detecting capability of some

central nervous system diseases with phagocytes involvement. In experimental encephalomyelitis, lesions had been seen by T2W MR imaging as low signal intensities after USPIO administration. Acute early lesions measuring only 100 μm in diameter could be detected. Electron microscopy revealed the presence of iron particles within the cytoplasm of macrophages at the lesion sites [56, 57].

Hauger et al. [58] reported the detection of kidney macrophage infiltration with USPIO-enhanced T2W MR imaging in a rat model of experimental nephropathy. A significant signal decrease was observed in the nephropathy kidneys after USPIO enhancement.

Recently Ruehm et al. [59] reported the possibility of imaging atherosclerotic plaque in rabbits aorta with AMI-277 enhancement. It was found that AMI-277 particles were phagocytosed by macrophages in atherosclerotic plaques and may lead to MR imaging-detectable signal change.

Experimental studies also demonstrated substantial uptake and transport by axons after intraneural injection of MIONs modified with a strong surface charge or covalently linked to neurotropic protein. Numerous Schwann cells and macrophages acquired large fractions of the injected agents. The nerves appeared on T2W MR images as hypointense structures [60, 61].

Application of superparamagnetic iron oxide agents for MR angiography

The main advantage of using blood pool agents for MR angiography is that it allows a longer acquisition time window and there is less interstitial background enhancement. Reports about studies with USPIO for MR angiography in humans have been published since 1996. Stillman et al. [25, 26] reported that AMI-277 improved visualization of renal artery lengths and right coronary artery. Mayo-Smith et al. [27] studied the aorta, the inferior vena cava and the portal vein in 16 patients before and 45 min after administration of AMI-227. All vessels showed significant enhancement at 45 min. There was no significant increase in noise or signal intensity of muscle after contrast.

It had been reported that the degree of experimental common carotid artery stenosis, determined by NC100150-enhanced MR angiography, did not differ significantly from digital subtraction angiography (DSA), whereas time of flight (TOF) and phase contrast (PC) MR angiography underestimated it [24]. The image quality of the NC100150-enhanced MR angiography was superior to both unenhanced TOF and PC MR angiography [24]. In the phase I clinical study reported by Taylor et al. [62], NC 100150 was given safely to 18 healthy subjects for coronary MR angiography enhancement. Coronary artery delineation was improved with no major adverse reactions. High-quality MR angiograms of the pulmonary vasculature had been obtained with NC100150 injection, permitting complete visualization and excellent delineation of central, segmental, and subsegmental arteries [63]. Following iatrogenic injury in the two animals, pulmonary hemorrhage was readily detected [64].

NC100150 was also tested in a gastrointestinal bleeding animal model. It was shown that all bleeding sites were readily detected and localized on MR images while contrast material accumulated in the intestines and peritoneal space. The extent of the bleeding can be determined with repeat data acquisitions [65].

Contrast enhanced MR angiography is also feasible with SHU 555A, a type of SSPIO with relatively smaller size [2].

Application of superparamagnetic iron oxide agents for tissue perfusion imaging

Because of their high susceptibility, bolus-injectable USPIO agents are very suitable as perfusion study agents. Gadolinium chelates have been used for perfusion study by dynamic susceptibility contrast imaging. However, to stay within the recommended dose limit of 0.3 mmol/kg, current Gd-based contrast agents can only be administered a limited number of times in doses necessary for perfusion imaging. This limits the possibility for serial measurements with short time periods. USPIO agents have a low toxicity and hence provide the possibility of repeated measurement.

Brain perfusion imaging and functional imaging

Dynamic USPIO-enhanced susceptibility imaging is able to detect ischemic cerebral injury at an early stage. Magnetic susceptibility effects of iron particles cause low signal in normally perfused cerebral tissue, whereas tissue with reduced or absent blood flow continues to give relatively high signal [66]. Reproducible and comparable perfusion measurements had been obtained by using NC100150 at a dose of 7 μmol Fe/kg and Gd-DTPA at a dose of 200 μmol/kg [19]. The utility of a steady-state technique for continuous measurement of relative cerebral blood volume during global transient ischemia and subsequent hyperemia had been demonstrated, which permits continuous, in vivo mapping of alterations in cerebral blood volume [67].

By sensitizing the signal to cerebral blood volume changes, SPIO agents may increase the sensitivity of MR imaging to physiological variations in cerebral blood volume, thus making it useful for brain function imaging [68, 69].

Myocardial perfusion imaging

Contrast agents may improve the detection of the myocardial infarction region when cardiac edema is minimal. Extracellular contrast media (CM) are sub-optimal perfusion markers, as these agents equilibrate rapidly throughout the interstitial space, thereby hampering the exact delineation of hypoperfused areas. Rozenman et al. [70] studied the effect of SPIO on myocardial T2W MR imaging with rat models. It was demonstrated that myocardial signal intensity decreased following SPIO infusion in normal hearts. The intensity remained constant in the rat heart transplants during coronary occlusion, both before and after the infusion of SPIO, and decreased upon reperfusion. There was a larger effect of SPIO in reperfused myocardium than in normal myocardium, suggesting the presence of ischemia-induced hyperemia. Thus the use of SPIO permits identification of normal, ischemic, and reperfused myocardium. By using T1W MR sequence, the effect of SPIO as T1 enhancing agents in the investigation of a myocardial perfusion defect has also been reported. Compared with normal myocardium, the ischemic myocardial region appeared as a lower and delayed enhancing area [71]. Absolute quantification of myocardial tissue perfusion has been performed in pigs with left coronary anterior descending branch stenoses using NC100150. A high absolute quantification correlation was found between MR perfusion imaging and microsphere quantification [72].

The feasibility of improving myocardial/blood pool contrast in MR cine images through use of NC100150 was tested in human subjects. Larger image intensity gradients at the endocardial border were expected to improve the capabilities of automated segmentation algorithms, reducing the uncertainty and need for manual editing [73].

Kidney perfusion imaging

The use of USPIO-enhanced MR imaging in assessing renal function has been studied by experiments. Trillaud et al. [74] studied first-pass intrarenal hemodynamics with USPIO-enhanced MR imaging of rabbit kidney. It was found that the intravascular progression of the USPIO particles could be visualized within the cortex, the outer and inner compartments of the medulla. The enhancement was reduced and delayed in the kidneys, with ligation of the lumbar ureter or embolization of the renal artery. USPIO-enhanced MR was also used in the rabbit model of glycerol-induced acute renal failure. In the acute renal failure kidneys, contrast enhancement in the outer and inner medulla was significantly less than in the normal kidneys [75].

Tumor vascularity perfusion

Tumor sprouted vessels can be greater in both number and diameter than in their healthy counterparts. This abnormal vascularity can be studied and quantified in vivo by SPIO-enhanced perfusion study.

The potential of T2/T2*W USPIO-enhanced MR imaging to characterize rat brain glioma vascularization has been evaluated. The $\Delta R2^*$ variations due to the injection of the contrast agent were used to generate relative cerebral blood volume [76]. Dennie et al. [77] reported that $\Delta R2^*/\Delta R2$ increases as vessel size increases, and can be used as a measure of the average vessel size within a region of interest (ROI) or a voxel. This ratio compared favorably with a predicted ratio calculated from histologically determined vessel sizes and theoretical modeling results. ($\Delta R2$ and $\Delta R2^*$ are the differences between T2 and T2* *relaxation rates*[4] pre- and post-contrast agent injection).

Human hepatocellular carcinoma vascularity was evaluated with SHU 555A-enhanced susceptibility-sensitive echoplanar sequences. Transient decreases in tumor signal intensity were seen in the perfusion phase. These decreases in signal intensity were different for poorly differentiated, moderately differentiated and well-differentiated hepatocellular carcinoma, with poorly differentiated tumors showing the strongest signal decreases and well-differentiated tumors showing the mildest signal decreases [78].

Superparamagnetic iron oxide agents for receptor-directed MR imaging and magnetically labeled cell probe MR imaging

Most receptor-directed agents and magnetically labeled cell probes use MIONs. MIONs can pass through capillary fenestra and inter-endothelial junctions to reach the extra-vascular space. This passage is a prerequisite for these targeted imagings.

The concept of development of a small superparamagnetic probe conjugated to antibody was first presented by Weissleder and colleagues [14, 15]. They attached MION to antimyosin Fab for immunospecific MR imaging of cardiac infarcts. A specific binding of the immunoconjugate to infarcted, but not to normal myocardium, was confirmed [14]. When polyclonal Ig G was attached to MION, MION-IgG caused enhancement at the site of an animal model of myositis [15].

[4] Relaxation rates R1 and R2 are the inverse of the T1 or T2 relaxation time. Relaxation rate are a useful concept for discussion of contrast agent effects, because, unlike relaxation times, relaxation rates from different sources can be directly added to assess their cumulative effect.

For tumor-specific imaging, monoclonal antibodies specific to carcinoembryonic antigen [79], epidermal growth factor receptors [4], human glioma cell-surface antigen [80], and other antigens [81, 82] have been attached to MION. Their efficacy has been established in ex vivo studies and animal studies.

The expression of tumor markers on tumor cell surfaces is not a static situation but changes with the evolution of the type and amount of antigen presented over time. An approach aiming at the highest possible specificity also bears a high risk of less sensitivity. The use of a less-specificity mechanism related to cell proliferation, such as angiogenesis-associated factors, has also been proposed. Human transferrin has been coupled to MION. A combination of the SPIO relaxivity properties with the specificity of transferrin-mediated endocytosis allowed in vivo detection of tumors by MR imaging [5].

MIONs have also been labeled with materials expressing high affinity for receptors of normal tissue cells. MION was attached to cholecystokinin for MR receptor imaging of normal rat pancreas. Bio-distribution studies showed a significant enhancement in pancreatic tissues but not in tumor after administration of this complex [83]. Arabinogalactan-coated MION and asialofetuin-coated MION target the contrast agent exclusively to hepatocytes. These agents can be used to assess focal hepatic lesions as well as haptocyte function [84, 85].

By incubation with a variety of cells with MIONs, these cells can be efficiently labeled with MION particles via endocytosis uptake [86, 87]. This technique may be used for MR imaging of in vivo cell tracking. Dynamic MR tracking of rat T-cells labeled with MION has been performed successfully in rat testicles, with tissue inflammation induced by the local injection of a calcium ionophore to attract T-cells [88]. MION-labeled neutrophils have also been tested as inflammation-specific contrast agents for MR imaging [6]. Uptake of SPIOs by neutrophils and monocytes and these cells' ability to aggregate in the inflamed site is related to the size and coating of the MIONs [89].

Conclusion

The introduction of SPIO agents opens up an important field of research for scientists, industries and clinical radiologists. AMI-25 enhanced MR imaging using T2/T2*W sequences following slow infusion of the contrast agent has been shown to improve the detection of focal liver lesions, compared with non-enhanced MRI and contrast-enhanced CT. Recently developed bolus-injectable SPIO agents such as SHU 555A enable more versatile approaches to be made for liver imaging by means of dynamic imaging. A combination of T1 and T2/T2*W imaging provides more useful information than T2/T2*W imaging alone. The clinical value of USPIO-enhanced lymph node MR imaging has been established; approval of these agents will lead to wide application for the diagnosis of lymph node metastasis. The blood pool property of the smaller SPIO agents may be used in MR angiography of difficult vessels such as coronary arteries, and in perfusion imaging. Though the final clinical relevance of receptor-directed MR imaging and magnetically labeled cell probe MR imaging remains far from established, these techniques may fundamentally change the practice of MR imaging, leading to the assessment of tissue function at the cell and molecular levels. However, further wider application of bowel contrast is not expected, due to intrinsic good soft tissue resolution of MR imaging with modern scanners. As extremely high doses were used in many experimental studies of RES imaging for diseases such as autoimmune encephalomyelitis and atherosclerotic plaque, the question of how these results can be extrapolated to humans remains uncertain [90].

The further development of SPIO-enhanced MR imaging depends on improved knowledge of the fundamental mechanism of SPIO agents on MR signals, and the pharmacokinetic control of these agents, including appropriate selection of particle charge, size and coating, linking these agents with molecules capable of accurate specific targeting, and development of new imaging sequences.

Acknowledgement The authors thank Andries Zwamborn for preparing the figures, Paul B Gordon of Nycomed Amersham and Wolfgang Ebert of Schering AG for their helpful advice.

References

1. Bach-Gansmo T (1993) Ferrimagnetic susceptibility contrast agents. Acta Radiol [Suppl] 387: 1–30
2. Reimer P, Tombach (1998) Hepatic MRI with SPIO: detection and characterization of focal liver lesions. Eur Radiol 8: 1198–1204
3. Grubnic S, Padhani AR, Revell PB, Husband JE (1999) Comparative efficacy of and sequence choice for two oral contrast agents used during MR imaging. Am J Roentgenol 173: 173–178
4. Suwa T, Ozawa S, Ueda M, Ando N, Kitajima M (1998) Magnetic resonance imaging of esophageal squamous cell carcinoma using magnetite particles coated with anti-epidermal growth factor receptor antibody. Int J Cancer 75: 626–634

5. Kresse M, Wagner S, Pfefferer D, Lawaczeck R, Elste V, Semmler W (1998) Targeting of ultrasmall superparamagnetic iron oxide (USPIO) particles to tumor cells in vivo by using transferrin receptor pathways. Magn Reson Med 40: 236–242
6. Krieg FM, Andres RY, Winterhalter KH (1995) Superparamagnetically labelled neutrophils as potential abscess-specific contrast agent for MRI. Magn Reson Imaging 13: 393–400
7. Bean CP (1955) Hysteresis loops of mixture of ferromagnetic micropowders. J Appl Physiol 26: 1381
8. Bean CP, Livingston JD (1959) Superparamagnetism. J Appl Physiol 30 [Suppl]:120S
9. Jung CW, Jacobs P (1995) Physical and chemical properties of superparamagnetic iron oxide MR contrast agents: ferumoxides, ferumoxtran, ferumoxsil. Magn Reson Imaging 13: 661–674
10. Weissleder R, Elizondo G, Wittenberg J, Rabito CA, Bengele HH, Josephson L (1990) Ultrasmall superparamagnetic iron oxide: characterization of a new class of contrast agents for MR imaging. Radiology 175: 489–493
11. Knollmann FD, Bock JC, Rautenberg K, Beier J, Ebert W, Felix R (1998) Differences in predominant enhancement mechanisms of superparamagnetic iron oxide and ultrasmall superparamagnetic iron oxide for contrast-enhanced portal magnetic resonance angiography. Preliminary results of an animal study original investigation. Invest Radiol 33: 637–643
12. Groman EV, Josephson L, Lewis JM (1989) Biologically degradable superparamagnetic materials for use in clinical applications. US patent 4827945, Section 7.1
13. Palmacci S, Josephson L (1993) Synthesis of polysaccharide covered superparamagnetic oxide colloids. US patent 5262176, example 1
14. Weissleder R, Lee AS, Khaw BA, Shen T, Brady TJ (1992) Antimyosin-labeled monocrystalline iron oxide allows detection of myocardial infarct: MR antibody imaging. Radiology 182: 381–385
15. Weissleder R, Lee AS, Fischman AJ, Reimer P, Shen T, Wilkinson R, Callahan RJ, Brady TJ (1991) Polyclonal human immunoglobulin G labeled with polymeric iron oxide: antibody MR imaging. Radiology 181: 245–249
16. Chouly C, Pouliquen D, Lucet I, Jeune JJ, Jallet P (1996) Development of superparamagnetic nanoparticles for MRI: effect of particle size, charge and surface nature on biodistribution. J Microencapsul 13: 245–255
17. Weissleder R, Bogdanov A, Neuwelt EA, Papisov M (1995) Long-circulating iron oxides for MR imaging. Adv Drug Del Rev 16: 321–344
18. Reimer P, Rummeny EJ, Daldrup HE, Balzer T, Tombach B, Berns T, Peters PE (1995) Clinical results with Resovist: a phase 2 clinical trial. Radiology 195: 489–496
19. Simonsen CZ, Ostergaard L, Vestergaard-Poulsen P, Rohl L, Bjornerud A, Gyldensted C (1999) CBF and CBV measurements by USPIO bolus tracking: reproducibility and comparison with Gd-based values. J Magn Reson Imaging 9: 342–347
20. Hahn PF, Stark DD, Lewis JM, Saini S, Elizondo G, Weissleder R, Fretz CJ, Ferrucci JT (1990) First clinical trial of a new superparamagnetic iron oxide for use as an oral gastrointestinal contrast agent in MR imaging. Radiology 175: 695–700
21. Weissleder R, Elizondo G, Josephson L, Compton CC, Fretz CJ, Stark DD, Ferrucci JT (1989) Experimental lymph node metastases: enhanced detection with MR lymphography. Radiology 171: 835–839
22. Weissleder R, Stark DD, Engelstad BL, Bacon BR, Compton CC, White DL, Jacobs P, Lewis J (1989) Superparamagnetic iron oxide: pharmacokinetics and toxicity. AJR Am J Roentgenol 152: 167–173
23. McLachlan SJ, Morris MR, Lucas MA, Fisco RA, Eakins MN, Fowler DR, Scheetz RB, Olukotun AY (1994) Phase I clinical evaluation of a new iron oxide MR contrast agent. J Magn Reson Imaging 4: 301–307
24. Rohl L, Ostergaard L, Simonsen CZ, Vestergaard-Poulsen P, Sorensen L, Bjornerud A, Saebo KB, Gyldensted C (1999) NC100150-enhanced 3D-SPGR MR angiography of the common carotid artery in a pig vascular stenosis model. Quantification of stenosis and dose optimization. Acta Radiol 40: 282–290
25. Stillman AE, Wilke N, Li D, Haacke M, McLachlan S (1996) Ultrasmall superparamagnetic iron oxide to enhance MRA of the renal and coronary arteries: studies in human patients. J Comput Assist Tomogr 20: 51–55
26. Stillman AE, Wilke N, Jerosch-Herold M (1997) Use of an intravascular T1 contrast agent to improve MR cine myocardial-blood pool definition in man. J Magn Reson Imaging 7: 765–767
27. Mayo-Smith WW, Saini S, Slater G, Kaufman JA, Sharma P, Hahn PF (1996) MR contrast material for vascular enhancement: value of superparamagnetic iron oxide. Am J Roentgenol 166: 73–77
28. Anzai Y, Blackwell KE, Hirschowitz SL, Rogers JW, Sato Y, Yuh WT, Runge VM, Morris MR, McLachlan SJ, Lufkin RB (1994) Initial clinical experience with dextran-coated superparamagnetic iron oxide for detection of lymph node metastases in patients with head and neck cancer. Radiology 192: 709–715
29. Anzai Y, Brunberg JA, Lufkin RB (1997) Imaging of nodal metastases in the head and neck. J Magn Reson Imaging 7: 774–783
30. Hudgins P, Anzai Y, Morris M (1996) Dextran-coated superparamagnetic iron oxide MR contrast agent (Combidex) for imaging cervical lymph nodes: optimal dose, time of imaging, and pulse sequence (abstract). Presented at the 1996, Los Angeles, American Society of Neuroradiology, Seattle, p 269
31. Saeed M, Wendland MF, Engelbrecht M, Sakuma H, Higgins CB (1998)Value of blood pool contrast agents in magnetic resonance angiography of the pelvis and lower extremities. Eur Radiol 8: 1047–1053
32. Reimer P, Tmbach B, Mahler M, Engehardt, M, A Renger B, Heindel, WL (2000) Preliminary experience of cardiac perfusion with a novel intravascular contrast agent (SHU 555C) in humans. ECR 2000 abstract book, p 129
33. Tombach B, Reimer P, Bremer C, Allkemper T, Engehardt M, Mahler M, Heindel, WL (2000) MRA with a new blood pool contrast agent: Phase I clinical trial. ECR 2000 abstract book, p 279
34. Lecesne R, Drouillard J, Cisse R, Schiratti M (1998) Contribution of Abdoscan in MRI cholangio-pancreatography and MRI urography (in French). J Radiol 79: 573–575
35. Bremer C, Allkemper T, Baermig J, Reimer P (1999) RES-specific imaging of the liver and spleen with iron oxide particles designed for blood pool MR-angiography. J Magn Reson Imaging 10: 461–467
36. Bartolozzi C, Lencioni R, Donati F, Cioni D (1999) Abdominal MR: liver and pancreas. Eur Radiol 9: 1496–1512
37. Seneterre E, Taourel P, Bouvier Y, Pradel J, Van Beers B, Daures JP, Pringot J, Mathieu D, Bruel JM (1996) Detection of hepatic metastases: ferumoxides-enhanced MR imaging versus unenhanced MR imaging and CT during arterial portography. Radiology 200: 785–792

38. Ros PR, Freeny PC, Harms SE, Seltzer SE, Davis PL, Chan TW, Stillman AE, Muroff LR, Runge VM, Nissenbaum MA, et al. (1995) Hepatic MR imaging with ferumoxides: a multicenter clinical trial of the safety and efficacy in the detection of focal hepatic lesions. Radiology 196: 481–488
39. Muller M, Reimer P, Wiedermann D, Allkemper T, Marx C, Tombach B, Rummeny EJ, Shamsi K, Balzer T, Peters PE (1998) T1-weighted dynamic MRI with new superparamagnetic iron oxide particles (Resovist): results of a phantom study as well as 25 patients (in German). Rofo Fortschr Geb Rontgenstr Neuen Bildgeb Verfahr 168: 228–236
40. Reimer P, Allkemper T, Matuszewski L, Balzer T (1999) Contrast-enhanced 3D-MRA of the upper abdomen with a bolus-injectable SPIO (SHU 555A). J Magn Reson Imaging 10: 65–71
41. Grangier C, Tourniaire J, Mentha G, Schiau R, Howarth N, Chachuat A, Grossholz M, Terrier F (1994) Enhancement of liver hemangiomas on T1-weighted MR SE images by superparamagnetic iron oxide particles. J Comput Assist Tomogr 18: 888–896
42. Harisinghani MG, Saini S, Weissleder R, Halpern EF, Schima W, Rubin DL, Stillman AE, Sica GT, Small WC, Hahn PF (1997) Differentiation of liver hemangiomas from metastases and hepatocellular carcinoma at MR imaging enhanced with blood-pool contrast agent Code-7227. Radiology 202: 687–691
43. Saini S, Edelman RR, Sharma P, Li W, Mayo-Smith W, Slater GJ, Eisenberg PJ, Hahn PF (1995) Blood-pool MR contrast material for detection and characterization of focal hepatic lesions: initial clinical experience with ultrasmall superparamagnetic iron oxide (AMI-227). AJR Am J Roentgenol 164: 1147–1152
44. Muhler A, Freise CE, Kuwatsuru R, Rosenau W, Liu T, Mintorovitch J, Clement O, Vexler V, Mahboubi S, Lang P, et al. (1993) Acute liver rejection: evaluation with cell-directed MR contrast agents in a rat transplantation model. Radiology 186: 139–146
45. Morimoto N, Ebara M, Kato H, Obata T, Fujita J, Kondo F, Tsujii H, Saisho H (1999) Early detection of radiation-induced liver injury in rat by superparamagnetic iron oxide-enhanced MR imaging. J Magn Reson Imaging 9: 573–578
46. Yamashita Y, Yamamoto H, Hirai A, Yoshimatsu S, Baba Y, Takahashi M (1996) MR imaging enhancement with superparamagnetic iron oxide in chronic liver disease: influence of liver dysfunction and parenchymal pathology. Abdom Imaging 21: 318–323
47. Kato N, Takahashi M, Tsuji T, Ihara S, Brautigam M, Miyazawa T (1999) Dose-dependency and rate of decay of efficacy of Resovist on MR images in a rat cirrhotic liver model. Invest Radiol 34: 551–557
48. Kreft BP, Tanimoto A, Leffler S, Finn JP, Oksendal AN, Stark DD (1994) Contrast-enhanced MR imaging of diffuse and focal splenic disease with use of magnetic starch microspheres. J Magn Reson Imaging 4: 373–379
49. Bellin MF, Roy C, Kinkel K, Thoumas D, Zaim S, Vanel D, Tuchmann C, Richard F, Jacqmin D, Delcourt A, Challier E, Lebret T, Cluzel P (1998) Lymph node metastases: safety and effectiveness of MR imaging with ultrasmall superparamagnetic iron oxide particles – initial clinical experience. Radiology 207: 799–808
50. Vassallo P, Matei C, Heston WD, McLachlan SJ, Koutcher JA, Castellino RA (1995) Characterization of reactive versus tumor-bearing lymph nodes with interstitial magnetic resonance lymphography in an animal model. Invest Radiol 30: 706–711
51. Seneterre E, Weissleder R, Jaramillo D, Reimer P, Lee AS, Brady TJ, Wittenberg J (1991) Bone marrow: ultrasmall superparamagnetic iron oxide for MR imaging. Radiology 79: 529–533
52. Axmann C, Bohndorf K, Gellissen J, Prescher A, Lodemann KP (1998) Mechanisms of accumulation of small particles of iron oxide in experimentally induced osteosarcomas of rats: a correlation of magnetic resonance imaging and histology. Preliminary results. Invest Radiol 33: 236–245
53. Bush CH, Mladinich CR, Montgomery WJ (1997) Evaluation of an ultrasmall superparamagnetic iron oxide in MRI in a bone tumor model in rabbits. J Magn Reson Imaging 7: 579–584
54. Daldrup HE, Link TM, Blasius S, Strozyk A, Konemann S, Jurgens H, Rummeny EJ (1999) Monitoring radiation-induced changes in bone marrow histopathology with ultra-small superparamagnetic iron oxide (USPIO)-enhanced MRI. J Magn Reson Imaging 9: 643–652
55. Vande Berg BC, Lecouvet FE, Kanku JP, Jamart J, Van Beers BE, Maldague B, Malghem J (1999) Ferumoxides-enhanced quantitative magnetic resonance imaging of the normal and abnormal bone marrow: preliminary assessment. J Magn Reson Imaging 9: 322–328
56. Dousset V, Delalande C, Ballarino L, Quesson B, Seilhan D, Coussemacq M, Thiaudiere E, Brochet B, Canioni P, Caille JM (1999) In vivo macrophage activity imaging in the central nervous system detected by magnetic resonance. Magn Reson Med 41: 329–333
57. Xu S, Jordan EK, Brocke S, Bulte JW, Quigley L, Tresser N, Ostuni JL, Yang Y, McFarland HF, Frank JA (1998) Study of relapsing remitting experimental allergic encephalomyelitis SJL mouse model using MION-46L enhanced in vivo MRI: early histopathological correlation. J Neurosci Res 52: 549–558
58. Hauger O, Delalande C, Trillaud H, Deminiere C, Quesson B, Kahn H, Cambar J, Combe C, Grenier N (1999) MR imaging of intrarenal macrophage infiltration in an experimental model of nephrotic syndrome. Magn Reson Med 41: 156–162
59. Ruehm SG, Corot C, Debatin JF (1999) MR imaging of atherosclerotic plaque with ultrasmall superparamagnetic iron oxide in hyperlipedemic rabbits. Radiology 213 [Suppl]:267
60. van Everdingen KJ, Enochs WS, Bhide PG, Nossiff N, Papisov M, Bogdanov A Jr, Brady TJ, Weissleder R (1994) Determinants of in vivo MR imaging of slow axonal transport. Radiology 193: 485–491
61. Petropoulos AE, Schaffer BK, Cheney ML, Enochs S, Zimmer C, Weissleder R (1995) MR imaging of neuronal transport in the guinea pig facial nerve: initial findings. Acta Otolaryngol (Stockh) 115: 512–516
62. Taylor AM, Panting JR, Keegan J, Gatehouse PD, Amin D, Jhooti P, Yang GZ, McGill S, Burman ED, Francis JM, Firmin DN, Pennell DJ (1999) Safety and preliminary findings with the intravascular contrast agent NC100150 injection for MR coronary angiography. J Magn Reson Imaging 9: 220–227
63. Ahlstrom KH, Johansson LO, Rodenburg JB, Ragnarsson AS, Akeson P, Borseth A (1999) Pulmonary MR angiography with ultrasmall superparamagnetic iron oxide particles as a blood pool agent and a navigator echo for respiratory gating: pilot study. Radiology 211: 865–869

64. Weishaupt D, Hilfiker PR, Schmidt M, Debatin JF (1999) Pulmonary hemorrhage: imaging with a new magnetic resonance blood pool agent in conjunction with breathheld three-dimensional magnetic resonance angiography. Cardiovasc Intervent Radiol 22: 321–325
65. Hilfiker PR, Zimmermann-Paul GG, Schmidt M, Klotz HP, Kacl GM, Debatin JF (1998) Intestinal and peritoneal bleeding: detection with an intravascular contrast agent and fast three-dimensional MR imaging – preliminary experience from an experimental study. Radiology 209: 769–774
66. Forsting M, Reith W, Dorfler A, von Kummer R, Hacke W, Sartor K (1994) MRI in acute cerebral ischaemia: perfusion imaging with superparamagnetic iron oxide in a rat model. Neuroradiology 36: 23–26
67. Hamberg LM, Boccalini P, Stranjalis G, Hunter GJ, Huang Z, Halpern E, Weisskoff RM, Moskowitz MA, Rosen BR (1996) Continuous assessment of relative cerebral blood volume in transient ischemia using steady state susceptibility-contrast MRI. Magn Reson Med 35: 168–173
68. Berry I, Benderbous S, Ranjeva JP, Gracia-Meavilla D, Manelfe C, Le Bihan D (1996) Contribution of Sinerem used as blood-pool contrast agent: detection of cerebral blood volume changes during apnea in the rabbit. Magn Reson Med 36: 415–419
69. van Bruggen N, Busch E, Palmer JT, Williams SP, de Crespigny AJ (1998) High-resolution functional magnetic resonance imaging of the rat brain: mapping changes in cerebral blood volume using iron oxide contrast media. J Cereb Blood Flow Metab 18: 1178–1183
70. Rozenman Y, Zou XM, Kantor HL (1991) Magnetic resonance imaging with superparamagnetic iron oxide particles for the detection of myocardial reperfusion. Magn Reson Imaging 9: 933–939
71. Canet E, Revel D, Forrat R, Baldy-Porcher C, de Lorgeril M, Sebbag L, Vallee JP, Didier D, Amiel M (1993) Superparamagnetic iron oxide particles and positive enhancement for myocardial perfusion studies assessed by subsecond T1-weighted MRI. Magn Reson Imaging 11: 1139–1145
72. Tarlo KS, Jerosch-Herold, Mansoor A, et al. (1999) NC100150 injection: a new intravascular MR contrast agent for morphological and functional assessment of the heart (abstract). J Cardiovasc Magn Reson 1: 65
73. Panting JR, Taylor AM, Gatehouse PD, Keegan J, Yang GZ, McGill S, Francis JM, Burman ED, Firmin DN, Pennell DJ (1999) First-pass myocardial perfusion imaging and equilibrium signal changes using the intravascular contrast agent NC100150 injection. J Magn Reson Imaging 10: 404–410
74. Trillaud H, Grenier N, Degreze P, Louail C, Chambon C, Franconi JM (19) First-pass evaluation of renal perfusion with TurboFLASH MR imaging and superparamagnetic iron oxide particles. J Magn Reson Imaging 3: 83–91
75. Trillaud H, Degreze P, Combe C, Deminiere C, Palussiere J, Benderbous S, Grenier N (1995) USPIO-enhanced MR imaging of glycerol-induced acute renal failure in the rabbit. Magn Reson Imaging 13: 233–240
76. Le Duc G, Peoc'h M, Remy C, Charpy O, Muller RN, Le Bas JF, Decorps M (1999) Use of T(2)-weighted susceptibility contrast MRI for mapping the blood volume in the glioma-bearing rat brain. Magn Reson Med 42: 754–761
77. Dennie J, Mandeville JB, Boxerman JL, Packard SD, Rosen BR, Weisskoff RM (1998) NMR imaging of changes in vascular morphology due to tumor angiogenesis. Magn Reson Med 40: 793–799
78. Ichikawa T, Arbab AS, Araki T, Touyama K, Haradome H, Hachiya J, Yamaguchi M, Kumagai H, Aoki S (1999) Perfusion MR imaging with a superparamagnetic iron oxide using T2-weighted and susceptibility-sensitive echoplanar sequences: evaluation of tumor vascularity in hepatocellular carcinoma. Am J Roentgenol 173: 207–213
79. Tiefenauer LX, Kuhne G, Andres RY (1993) Antibody-magnetite nanoparticles: in vitro characterization of a potential tumor-specific contrast agent for magnetic resonance imaging. Bioconjug Chem 4: 347–352
80. Suzuki M, Honda H, Kobayashi T, Wakabayashi T, Yoshida J, Takahashi M (1996) Development of a target-directed magnetic resonance contrast agent using monoclonal antibody-conjugated magnetic particles. Noshuyo Byori 13: 127–132
81. Remsen LG, McCormick CI, Roman-Goldstein S, Nilaver G, Weissleder R, Bogdanov A, Hellstrom I, Kroll RA, Neuwelt EA (1996) MR of carcinoma-specific monoclonal antibody conjugated to monocrystalline iron oxide nanoparticles: the potential for noninvasive diagnosis. Am J Neuroradiol 17: 411–418
82. Cerdan S, Lotscher HR, Kunnecke B, Seelig J (1989) Monoclonal antibody-coated magnetite particles as contrast agents in magnetic resonance imaging of tumors. Magn Reson Med 12: 151–163
83. Reimer P, Weissleder R, Shen T, Knoefel WT, Brady TJ (1994) Pancreatic receptors: initial feasibility studies with a targeted contrast agent for MR imaging. Radiology 193: 527–531
84. Schaffer BK, Linker C, Papisov M, Tsai E, Nossiff N, Shibata T, Bogdanov A Jr, Brady TJ, Weissleder R (1993) MION-ASF: biokinetics of an MR receptor agent. Magn Reson Imaging 11: 411–417
85. Leveille-Webster CR, Rogers J, Arias IM (1996) Use of an asialoglycoprotein receptor-targeted magnetic resonance contrast agent to study changes in receptor biology during liver regeneration and endotoxemia in rats. Hepatology 23: 1631–1641
86. Weissleder R, Cheng HC, Bogdanova A, Bogdanov A Jr (1997) Magnetically labeled cells can be detected by MR imaging. J Magn Reson Imaging 7: 258–263
87. Schulze E, Ferrucci JT Jr, Poss K, Lapointe L, Bogdanova A, Weissleder R (1995) Cellular uptake and trafficking of a prototypical magnetic iron oxide label in vitro. Invest Radiol 30: 604–610
88. Yeh TC, Zhang W, Ildstad ST, Ho C (1995) In vivo dynamic MRI tracking of rat T-cells labeled with superparamagnetic iron-oxide particles. Magn Reson Med 33: 200–208
89. Chan TW, Eley C, Liberti P, So A, Kressel HY (1992) Magnetic resonance imaging of abscesses using lipid-coated iron oxide particles. Invest Radiol 27: 443–449
90. Dousset V, Gomez C, Petry KG, Delalande C, Caille JM (1999) Dose and scanning delay using USPIO for central nervous system macrophage imaging. MAGMA 8: 185–189